Soft Matter

Accepted Manuscript

ROYAL SOCIETY OF CHEMISTRY

www.rsc.org/softmatter

Cite this: DOI: 10.1039/c0xx00000x

www.rsc.org/xxxxxx

PAPER

Viscoelastic changes measured in partially suspended single bilayer membranes

Imad Younus Hasan[a] and Adam Mechler*[a]

Received (in XXX, XXX) XthXXXXXXXXX 20XX, Accepted Xth XXXXXXXXX 20XX

DOI: 10.1039/b000000x

For studies involving biomimetic phospholipid membrane systems, such as membrane-protein interactions, it is crucial that the supported membrane is biomimetic in its physical properties as well as in its composition. Two often overlooked aspects of biomimicry are the need for unrestrained lipid mobility, reflected in the viscoelastic properties of the membrane, and sufficient space between the membrane and the support for the insertion of transmembrane proteins. Here we show for a series of DMPC-based membranes, that a partially suspended single bilayer membrane can be formed on functionalized gold surface without tethering. These membranes exhibit sufficient freedom of motion to represent the viscoelastic properties of a free lamellar bilayer membrane as demonstrated by determining the phase transition temperatures of these single bilayer membranes from the viscosity change upon chain melting using the dissipation signal of a quartz crystal microbalance (QCM-D). Atomic force microscopy imaging confirmed confluent, smooth membrane coverage of the QCM-D sensor that completely obscured the roughness of the sputtered gold surface. High-force AFM imaging was able to push membrane patches into the valleys of the gold morphology, confirming the inherently suspended nature of the MPA supported membrane. We show that the correlation between frequency and dissipation changes in the QCM-D sensograms is a sensitive indicator of the morphology of the membrane.

Introduction

Membrane-protein interactions are frequently studied in a biomimetic environment provided by a supported phospholipid membrane.[1-5] Supported lipid membranes are usually created via liposome deposition due to the ease and simplicity of this methode.[6, 7] Planar lipid bilayers may form *via* spontaneous fusion of liposomes on both hydrophilic [8-11] and hydrophobic surfaces.[12-14] However, controlling the structural properties of the resulting membranes is often problematic. Several studies attempted to characterize the liposome deposition process to optimize and generalize the fusion mechanism[15-18]. Imaging assays provided snapshots of the surface binding and subsequent collapse of liposomes composed of various mixtures of zwitterionic, negatively charged and positively charge lipids on atomically smooth silica and mica surfaces [17, 19]. While the resulting membranes are typically smooth and defect free, membrane embedded semi-collapsed liposomes were also stable and robust enough to be imaged with AFM, and islands of membrane multilayers are often present. Furthermore, AFM imaging also revealed that flat lamellar membranes are not always homogeneous: mixtures of phosphatidylcholine and phosphatidylglycerol are prone to domain separation[20-25]. Thus, even in the absence of any unopened liposomes, supported membranes can be inhomogeneous.

To be useful for studying fine details of protein-membrane interactions, the biomimetic membrane should not only be structurally homogeneous but it should also faithfully represent key physicochemical properties of the plasma membrane, primarily its native viscoelasticity and phase transition temperature. Adhesion to the atomically smooth substrates used for imaging studies may restrict lipid mobility in the lower leaflet, leading to mechanical anisotropy. Quartz Crystal Microbalance with Dissipation (QCM-D) has been used to measure the viscoelastic properties of supported membranes (change in dissipation) simultaneously to the deposited mass (mostly reflected in frequency shift). Correlating the two signals also reveals changes in membrane structure upon environmental stimuli.[26] The majority of QCM-D works on vesicle fusion describe supported membranes as non-dissipative systems, which suggests that lipid mobility in the supported membranes is severely restrained due to strong surface binding [15, 17, 27]. Surface adhesion, and thus the chemical nature of the surface also plays an important role in the deposition process itself. On SiO_2 surfaces the deposition proceeds *via* fast mass uptake followed by a collective rupture of liposomes, to yield a final frequency shift of ~ -25Hz with baseline dissipation at the end of the process, which is used in the literature as a reference value to confirm bilayer formation [15, 16, 18]. However on TiO_2, oxidized Pt and oxidized gold surfaces the "rupture" step is absent: vesicles adsorb intact at all coverages and at temperatures both below and high above the phase transition temperature[15, 16]. Using

functionalization with 3-mercaptopropionic acid (MPA) self-assembled monolayer to alter the surface chemistry of gold, liposome deposition proceeds without a threshold, reaching final values of Δf = ~13 Hz and a relatively high dissipation of ΔD = 3.8 x 10^{-6} that was interpreted as a gradual process of surface binding, flattening and fusion of individual liposomes into a single bilayer membrane.[23, 28, 29] This interpretation was supported by modelling the viscoelastic properties of the deposits formed on the surface (adlayers). Importantly, only in this latter case is it possible to use the dissipation signal for extracting mechanistic detail from the real time recording of the interaction of proteins with the membrane, whereas under the tightly coupled bilayer conditions on SiO_2 QCM-D provides the same information as a traditional QCM. Optimally, the higher dissipation should reflect a weaker coupling of the membrane to the surface with substantial freedom of motion.

There is a further advantage to weak surface coupling of supported membranes. A key, but often overlooked requirement towards supported biomimetic membranes is to accommodate the cytoplasmic as well as extracellular domains of the proteins, that is, the need for an aqueous reservoir between the support surface and the bilayer membrane[30, 31].To this end, a variety of spacers has been suggested to suspend the membranes on the support surface, such as polymer cushions [32], polar peptides [33, 34], self assembled monolayer of oligoethylene glycol thiolates [35] as well as inert proteins [36, 37]. These spacers provide an irregular support, and the quality and morphology of bilayers formed on them is hard to characterize. Chemically tethered bilayer membranes have also been described, based on e.g. maleimide-thiol coupling chemistry[38] as well as modification of the lipid headgroups with a thiol [39], disulfide [40] or silane [41] functional group depending on the chemical composition of the substrate. Tethering provides sufficient space between the substrate and the lower part of the membrane to minimize interactions of the protein with the substrate and add extra degree of freedom which enhance the biomimetic character of the lipid bilayer.[42] However, the need for chemical modification of the lipid molecules reduces the practicality of the method, and the presence of "anchors", surface-bound non-moving molecules in the highly fluid membrane has a strong influence on the mass and viscosity of the resulting membranes as it was shown *via* QCM-D experiments[2, 39] Therefore there is a need for designing partially suspended membranes that are simple to deposit and easy to characterize; ideally, it should be a method to form suspended membranes on a QCM-D sensor chip surface to use the dissipation signal to analyze the quality of deposited membranes, as well as protein-membrane interactions on membranes of known biomimetic characteristics. We chose to study DMPC based membranes, mixed with either the more hydrophylic DMPG or the more hydrophobic cholesterol. The physicochemical properties of these mixtures, including their phase diagrams, are well understood[43, 44] and hence they are frequently used for biophysical characterization of protein and antimicrobial peptide function[23, 45-48].

Materials and Methods

Buffer preparation

Sodium chloride (NaCl) was obtained from Merck. Potassium dihydrogen phosphate (KH_2PO_4) and dipotassium hydrogen phosphate (K_2HPO_4) were purchased from Fluka (Switzerland) at ACS Reagent grade. For all solutions ultrapure water was used with a resistivity of 18.2MΩ (Ultrapure, Sartorius AG, Germany). The buffer solution used in this work contained 20mM phosphate and 100mM of NaCl at a pH 6.59

Preparation of Liposomes

1,2-Dimyristoyl-sn-Glycero-3-Phosphocholine (DMPC), 1,2-Dimyristoyl-sn-Glycero-3-Phospho-rac-1-glycerol (sodium salt) (DMPG) and cholesterol were purchased from Avanti Polar Lipids (Alabaster, AL, USA). Chloroform (ACS Reagent, 99.8%) was purchased from Sigma–Aldrich (Castle Hill, NSW, Australia). Individual stock solutions were created by dissolving dry DMPC, DMPG and cholesterol in chloroform. These stock solutions were then aliquot into test tubes in the desired ratios: DMPC, DMPC/ DMPG (4:1) as well as DMPC with 3%, 5%, 7%, 10% and 15 % cholesterol content. The solvent was evaporated under a gentle stream of nitrogen gas and placed in a desiccator overnight. Lipids were resuspended in 20 mM PBS which contain 100 mM of NaCl at pH 6.9 for 30min at 37°C. Before introducing the lipid suspensions to the QCM chambers, the suspensions were vortexed and briefly sonicated. This protocol yields liposomes of a broad size distribution which was found to promote vesicle fusion on the sensor chip surface.

Chip cleaning and surface modification

Hydrogen peroxide (H_2O_2), ammonia solution (28%, analytical Univar Reagent) and propan-2-ol were purchased from Sigma-Aldrich (Castle Hill, NSW, Australia). 3-Mercaptopropionic acid (MPA) (HPLC Grade, >99%) was purchased from Fluka (Switzerland). To clean the chip surfaces, the chips were placed into 1:1:3 mixture of ammonium hydroxide (28%), hydrogen peroxide (50%) solutions and water, at 70°C for 15–20 min. After that the chips were thoroughly rinsed with Ultrapure water and propan-2-ol (isopropanol). The clean chips were placed in MPA solution in isopropanol overnight to give sufficient time for the formation of a self-assembled monolayer on the gold surface. After functionalization the chips were rinsed with isopropanol and dried under a gentle stream of nitrogen gas. Functionalized chips were immediately assembled into the QCM chamber ready to use.

Quartz crystal microbalance experiments

All experiments were performed using a Q-SENSE E4 system (Q-SENSE-Sweden) using AT-cut gold coated quartz sensors (chips) with a fundamental resonance frequency of 5MHz. The frequency shift (Δf) and energy dissipation (ΔD) were recorded simultaneously at five overtones (3, 5, 7, 9 & 11th) corresponding to 15, 25, 35, 45 and 55 MHz, respectively. However, all values reported in this work for Δf and ΔD are that of the 7th overtone (35 MHz) unless stated otherwise. The raw data was analysed by QTools (Q-SENSE) and OriginPro 9 (Origin Lab, USA) softwares. All the deposition experiments were performed by pumping 1 mL of the liposome suspension (containing 10 µmole lipid) through the QCM cell at 50 µL/min flow rate followed by rinsing with buffer solution until a stable (constant) signal was reached for frequency and dissipation. For all temperature sweeping experiments the following programme was used: i) the

system was equilibrated at 15 °C for 30 min; ii) temperature was increased slowly at a rate of 0.33°C min^{-1} to 35°C; iii) the system was equilibrated for 30 min; and iv) temperature was returned to 15°C at a rate of 0.33°C min^{-1} followed by 30 min equilibration.

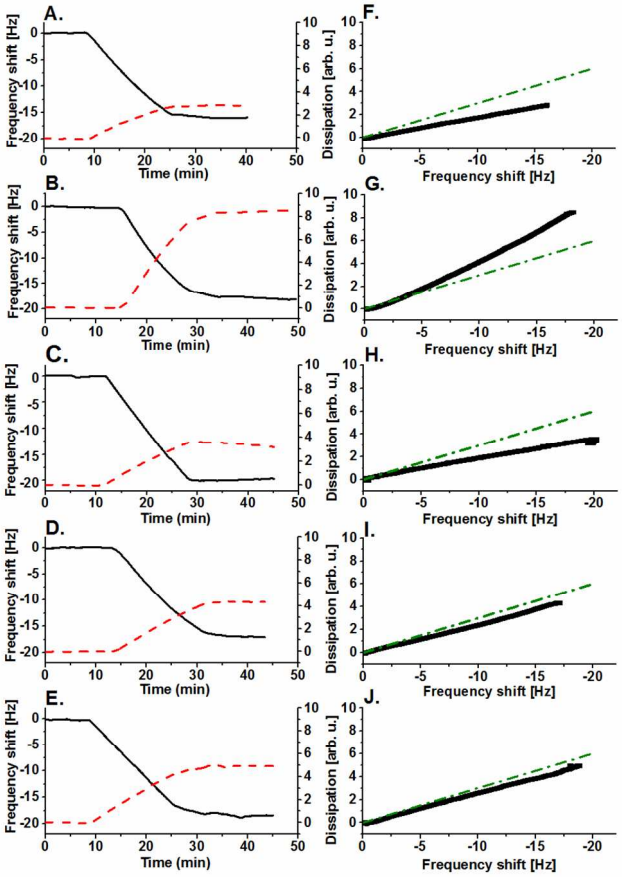

Fig.1 QCM sensograms of membrane deposition. A-E Frequency change (Δf; solid black line) and dissipation change (ΔD; dash red line) against time. F-J The same sensograms plotted as ΔD against -Δf (F-D curve). A: DMPC; B: DMPC:DMPG 4:1; C: DMPC: cholesterol 95:5;D: DMPC: cholesterol 9:1; E: DMPC: cholesterol 85:15.Dissipation values are divided by 10^{-6} in respect to raw data. In the right panels, green dot-dash line indicates the empirical deposition trendline for the formation of a homogeneous DMPC bilayer at 19°C.

Atomic force microscopy

QCM chips were imaged with AFM using an NT-MDT Ntegra platform (NT-MDT, Zelenograd, Russia), in scan-by-sample configuration, in a liquid cell, with µMasch NSC36B probes (90 µm long, nominal apex radius 10nm, resonance frequency under water is 60-100 kHz), in intermittent contact mode. QCM chips were removed from the QSense instrument after membrane deposition, and transferred in hydrated state into the AFM liquid cell. Images were taken immediately.

Differential Scanning Calorimetry

Experiments have been performed in a SETARAM µDSC Evo3 instrument, using 700 µl hastelloy pressure cells, recording three zones of the same parameters. Temperature profile was the same as the QCM temperature ramping experiments. 50µmol lipid suspended in PBS was introduced into the batch cell against a reference of the same volume of PBS.

Results and discussion

Formation of supported phospholipids bilayers

First, we attempted to identify the origin of different Δf and ΔD readings reported for phospholipid layers on MPA modified gold compared to SiO_2 substrates. QCM was used to monitor the deposition of liposomes onto MPA modified gold surface. Fig. 1 A shows the Δf and ΔD sensograms for the deposition of neat DMPC. The initial baseline between 0 and 500 seconds corresponds to the buffer in the measurement chamber in contact with the carboxylic acid-terminated MPA layer on the chip surface. At 500 s the lipid solution is injected resulting in a linear decrease in Δf and a concomitant increase in dissipation. The speed of the change in Δf and ΔD gradually decreases over time, and the two signals reach stable, constant values at Δf ≈ 16 Hz and ΔD ≈ 2.78 , respectively, which is not changed after washing with PBS.

Sensograms for DMPC: DMPG 4:1 mixture (Fig. 1 B) and DMPC: Cholesterol mixtures (Fig. 1 C-E) show very similar trends to neat DMPC deposition. For DMPC: DMPG 4:1 mixture Δf and ΔD reach stable values at ≈17.5 Hz and 8.45, respectively, while in case of DMPC: Cholesterol 95:5 the stable Δf and ΔD values are ~19 Hz and 3.5, respectively, even after rinsing with buffer for several minutes. Importantly, increasing the amount of cholesterol in the membrane resulted in a gradual shift in the final values of ΔD: ~4.35, and ~5, respectively, for 10% and 15 % cholesterol content.

The sensograms only reveal slight differences between the three lipid mixtures in the final values of Δf and ΔD. However, plotting ΔD against Δf (F-D curve) offers an additional insight into the mechanism of the deposition process. According to the continuum mechanic theory of QCM-D operation, layer thickness is a linear factor in both Δf and ΔD and thus deposition of a homogeneous layer should give a straight line in Δf-ΔD coordinates[49]. The slope of this line is dependent on viscosity and thus temperature; for dimyristoyl lipids at 19°C it is ~0.3 (dash-dot lines in Figure 1 right panels)[23]. At higher temperatures, such as in this work, the dissipation is lower and thus the slope of the line is less steep. Importantly, a slope larger than 0.3 may indicate the presence of highly dissipative unopened liposomes, while arching of the line reveals inhomogeneity during the deposition process, such as delayed rupture of liposomes.

In case of neat DMPC, the F-D curve shows a straight line with a slope of ~0.17 (Fig. 1 F), consistent with homogeneous deposition of a single bilayer membrane. The mixture containing DMPG exhibits a steeper slope (0.5) and arching towards higher D values, suggesting unopened liposome content (Fig. 1 G). The addition of cholesterol does not alter the linear trend at any mixing ratios, revealing a homogeneous deposition process. Importantly, the slope becomes steeper with increasing cholesterol content from 5% to 10% and 15%, respectively (Fig. 1 H-J), consistent with reports of increasing membrane viscosity as a function of cholesterol content[50-52].

Phase transitions in supported phospholipids bilayers

Assuming that the deposits are mostly fused lamellar membranes; the magnitude of the dissipation signal has to be dominated by the effect of the viscosity of the lipid bilayer. In this case,

different thermodynamic phases of the membrane might be distinguished by their different viscosities, that is, a difference in the dissipation signal.

Changes in the frequency and energy dissipation were monitored by the QCM-D upon temperature ramping. For all temperature sweeping experiments, a reference measurement chamber was used to carefully control for temperature-induced changes in the bulk solution.

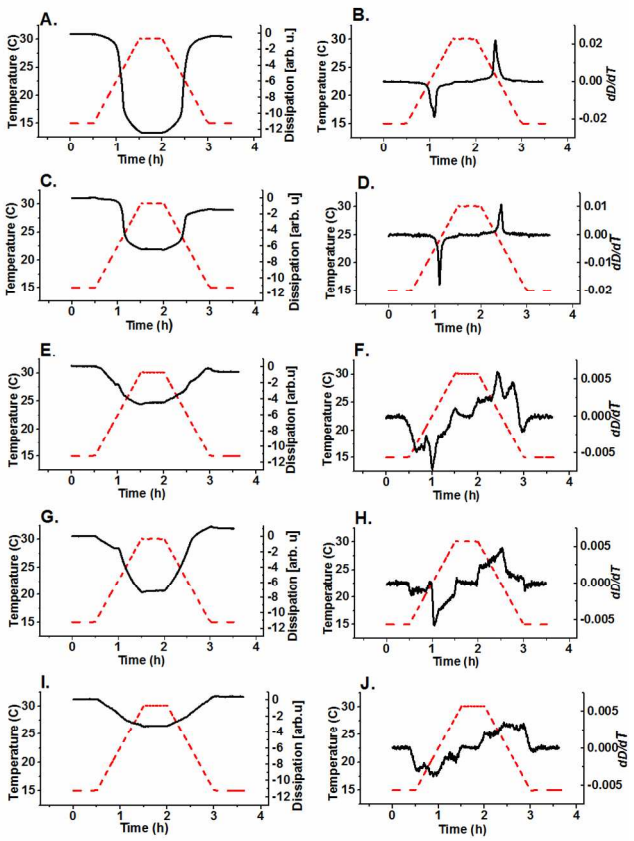

Fig.2 QCM sensograms of temperature scanning. Left panels: dissipation change (solid black line) and temperature (dash red line) against time. Right panels: The first derivatives of the dissipation signals displayed on the left panels; A,B: DMPC; C,D: DMPC:DMPG 4:1; E,F: DMPC: cholesterol 95:5; G,H: DMPC: cholesterol 9:1; I,J: DMPC: cholesterol 85:15.

Fig. 2a depicts the effect of temperature ramping on the dissipation signal in case of a neat DMPC bilayer. The red dashed line indicates the temperature profile, black solid line is the dissipation change. At constant 15°C temperature the dissipation signal was constant; this value was chosen as arbitrary zero. The temperature sweep starts at 30 min. Initially the dissipation change is slow, until the temperature reaches ~23°C where a steep change starts that is the fastest at ~24°C; after ~25°C the change gradually slows down until the sweep reaches its maximal value at 35°C. The negative temperature sweep mirrors the trend of the positive sweep with a slight hysteresis. In order to identify at which temperature is the dissipation change the steepest, the first derivative of dissipation (dD/dT) was plotted against time (Fig. 2 B). The plot shows two well defined peaks at 24.04°C and 23.3°C, for the positive and negative sweeps, respectively, giving a phase transition temperature of 23.67°C. Applying the same temperature profile to a bilayer of DMPC: DMPG (4:1) mixture leads to a similar profile, albeit the dissipation change is approximately half of that observed for neat DMPC membrane (Fig 2C). The first derivative shows two sharp peaks observed at 24.15°C for ramping up and at 23.76°C for ramping down the temperature, averaging to 23.95°C. Importantly, both of these values are accurately matched by DSC phase transition measurements performed on liposome suspensions of the same lipid mixtures (DMPC: 23.66°C, DMPG:DMPC (4:1): 23.96°C). DSC curves are shown in Supplementary Information (Fig. S1). Results are summarized in Table 1.

Table1: Phase transition temperatures of different lipid mixtures. QCM-D results for DMPC:cholesterol mixtures are approximations due to the lack of a clearly defined transition.

	QCM-D	DSC	literature
DMPC	23.67°C	23.66°C	23.6±1.5°C [53]
DMPC:DMPG 4:1	23.95°C	23.97°C	24.4 °C[54]
DMPC:cholesterol 3%	~22.96°C	23.31°C	~23.5±0.1°C[55]
DMPC:cholesterol 5%	~23.31°C	23.37°C	~23.3°C[56]
DMPC:cholesterol 7%	~23.21°C	22.91°C	~23.13°C[56]
DMPC:cholesterol 10%	~21.5°C	--------	~22.9°C[56]
DMPC:cholesterol 15%	---------	-------	~22.5°C[56]

In contrast to the neat DMPC and DMPC:DMPG 4:1, addition of cholesterol to the DMPC membrane resulted in the disappearance of the clear change of dissipation upon temperature ramping. Fig. 2E and G show that there is a near linear decrease of the dissipation signal while increasing the temperature from 15°C until ≈22°C, at which point the slope of dissipation change alters while still following a nearly linear trend. The negative temperature sweep mirrors this trend with the switching point at ≈21°C. The first derivative of the dissipation change shows a two step process for DMPC:cholesterol mixtures up to 10% cholesterol content (Fig. 2F,H; Table 1); the main peaks in these cases correspond well to the phase transition temperatures quoted in the literature (Table 1). Notably, the DSC measurement failed to show any discernible peaks for 10% and 15% cholesterol content at the same lipid concentration, while in the literature there are phase transition temperatures for these mixtures, measured in pure water[56]. This is consistent with literature evidence that the presence of cations in the aqueous environment has a strong influence on membrane phase behaviour[57]. Remarkably, in case of 15% cholesterol content the QCM-D dD/dT plots also fail to show a clear phase transition peak.

It is important to note that the dissipation signal of neat DMPC returned to the starting value after temperature ramping whereas in case of DMPC:DMPG 4:1 and DMPC:cholesterol 9:1 it did not, suggesting that the temperature ramping effected structural changes in the membrane, such as the removal of embedded liposomes. The magnitude of the difference was small, thus it is feasible to assume that the deposits predominantly consisted of bilayer membrane in these cases as well.

AFM results

An AFM image of the MPA modified gold surface is shown in Fig. 3 A. The morphology is uneven, consisting of broad, round,

flattened structures, characteristic of sputtered gold surfaces (e.g.[58]). In contrast, the membrane coated surface (Fig. 3 B; approximately a single bilayer membrane as per Mechler et al. [23]) is much smoother; ripples appearing on the surface are likely caused by lateral drag forces during imaging. Importantly, on the AFM images there is no sign of any unopened liposomes, and the outline of the gold particles is not distinguishable either. A comparison of the height profiles of the two surface morphologies is shown in Fig. 3 panel E, also revealing a smoother surface for the lipid coated sensor chip. *In situ* fluorescence microscopy imaging of membranes deposited from dye loaded liposomes on QCM sensor chip surface (Fig. S2) also confirmed the homogeneous membrane coverage and nearly total absence of unopened liposomes. When imaging a partially covered surface (Fig. 3 C; approx. 5Hz frequency change upon lipid deposition), the images show a more uneven surface however with much smaller roughness than the sputtered gold. A cross section along the white horizontal line is plotted in Panel F (red). The morphology confirms the absence of unopened liposomes; thus the surface bound membrane in this case has to be tightly bound, following the surface morphology. However, reducing the imaging force by increasing the setpoint amplitude leads to a remarkable change (Fig. 3 D and G): now flat islands are observed on the surface which exhibit a thickness of ~5nm according to the line section (Fig. 3 F), consistent with the thickness of a lipid bilayer. These islands appear to be suspended on the tallest peaks of the gold grains, which are clearly visible in areas where there is no membrane coverage.

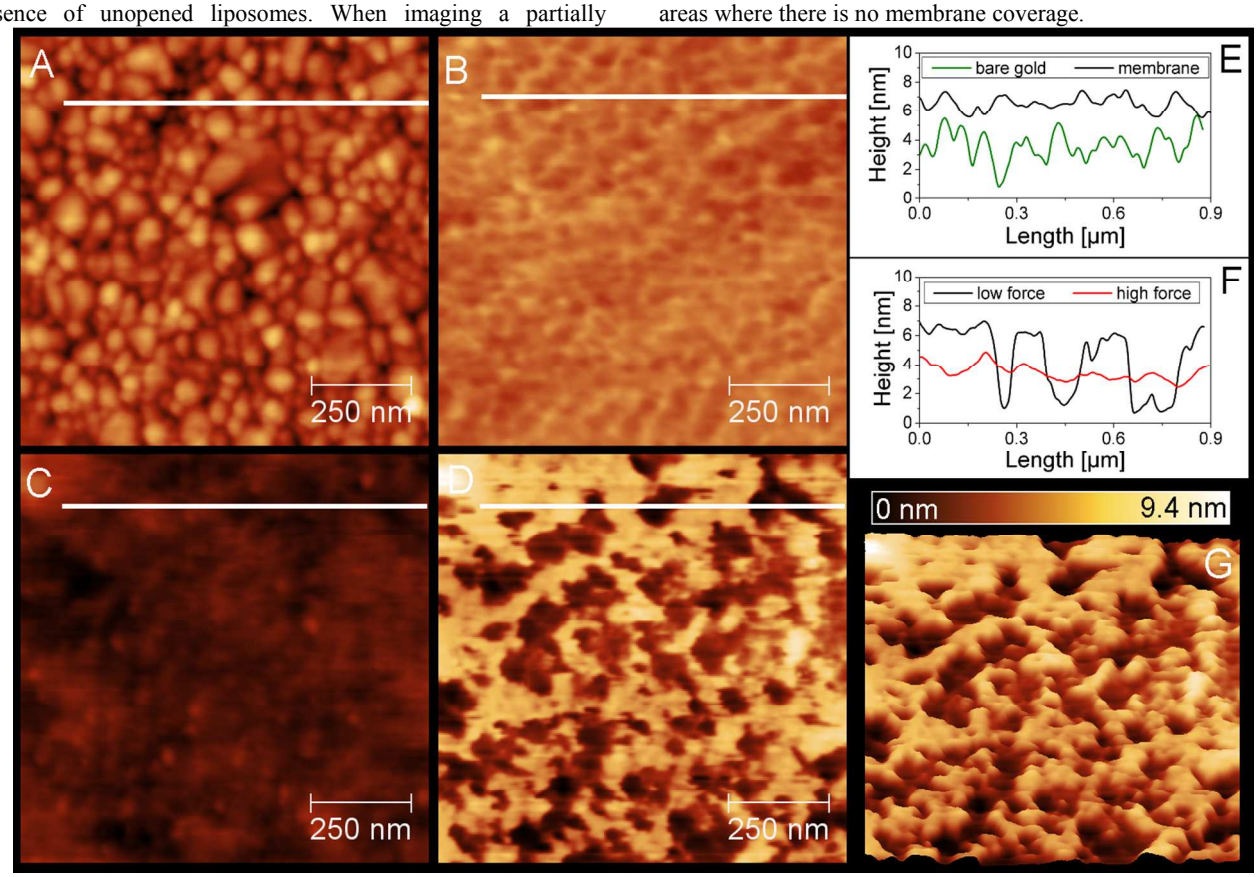

Fig. 3 AFM images of the QCM sensor surface A) before membrane deposition; B) after deposition of DMPC membrane at full coverage; C) partial coverage (<~50%) imaged with high tapping force; D) partial coverage (<~50%) imaged with low force; E) cross sections along the lines in (A) and (B); F) cross sections along the lines in (C) and (D); G) 3D rendered representation of (D). The colour scale covers a height of 9.4 nm and is the same for all images.

Formation of a supported phospholipid bilayer

AFM imaging suggests that the membrane on the chip surface is partially suspended, resting only on the tallest gold particles (Fig. 4 A). However, in case of partial coverage, the probe can force the membrane into the valleys of the surface morphology (Fig. 4 B). Importantly, reducing the imaging force allows the membrane to relax into a flat morphology that is suspended on the peaks of the substrate as it is clearly visible in Fig. 3 D&G. It is feasible to assume that, at least on MPA modified gold, the suspended form is the natural state of the membrane which is more resilient to imaging force in case of full coverage, when the water cannot escape from below and thus the membrane resists even higher imaging force.

Partial suspension of the membrane explains the differences in the "mass" (frequency shift) of lipid deposits measured with QCM-D as reported in the literature. The frequency shift of a single bilayer membrane is widely accepted to be -25Hz [5, 16, 59]. The Δf values of the confluent liposome layers before rupture[15, 16, 18] and the stable liposome layers [15, 16] typically exhibit a much higher frequency shift of ~-70-80 Hz. In contrast, in our study the frequency shift of a stable deposit is -16-18 Hz, a clear

indication of a structural difference. When comparing the dissipation signal to the literature data, for SiO_2 surfaces a near zero dissipation change has been reported, as outlined above; in case of liposome layers, the reported dissipation values of ~$3*10^{-6}$ correlate well to the values ($2.7\text{-}8.5*10^{-6}$) observed in this work. For a confluent layer of SUVs, typically ~20 nm diameter[15], the roughness would not be appreciably different from the substrate surface. Hence it is feasible to assume that in a tightly packed liposome layer the dissipation is dominated by the viscoelastic properties of the lamellar membrane through the deformations (compression, undulations) of the contacting liposomes in response to the crystal vibrations, rather than the drag of these liposomes in the liquid environment.

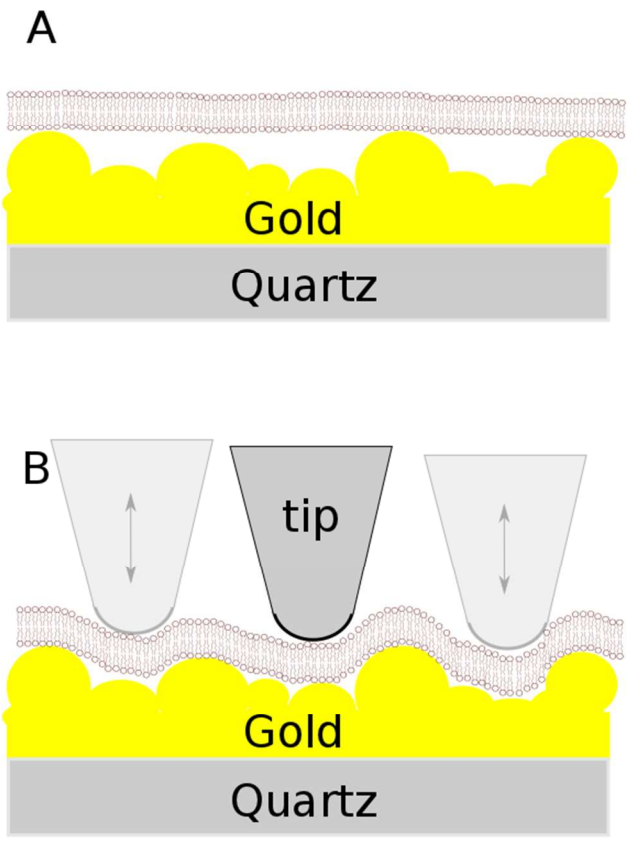

Fig. 4 Schematics of supported membrane (A) suspended on the gold grains and (B) pushed into the valleys of the morphology by the AFM probe

Therefore a partially suspended bilayer, as shown in the AFM images, may exhibit the same viscoelastic properties as a confluent layer of intact liposomes. The suspension, and thus the weaker coupling to the underlying substrate explains the lower frequency shift measured in these cases when compared to the literature, whereas the increased freedom of motion of the membrane allows for additional dissipative mechanisms (undulations, pressure waves) compared to the tightly bound supported membranes. The feasibility of creating a partially suspended membrane on a purposefully structured surface has been demonstrated before.[60] However, this report is the first observation of the spontaneous formation of a partially suspended membrane on a nanostructured surface.

To explain the formation of the partially suspended membrane the conditions and pathways of the deposition mechanism needs to be evaluated. The deposition process is clearly different to the thresholded mechanism reported by Keller et al. [15], and is more likely to proceed *via* immediate collapse and rupture upon surface binding, as it was suggested by Seantier et al.[5] for deposits forming from low lipid concentrations (≤ 0.01 mg/mL). In the same article[5] it was reported that this monotonous deposition "pathway" switches to a thresholded process once the lipid concentration is increased (≥0.01 mg/mL). Given that the parameters of the membrane produced by these two pathways are identical, it is equally feasible to assume that the underlying process is the same and an apparent threshold is observed when the time needed to saturate the surface with liposomes is shorter than the time needed for individual liposomes to rupture once on the surface. Thus, while the concentration in our study is similar to the one reportedly giving threshold-free bilayer deposition, we argue that the lipid concentration itself is unlikely to affect the mechanism of deposition, whereas the chemistry and morphology of the substrate are deterministic to the outcome of the deposition process. Most literature reports that include QCM characterization use silicon dioxide coated surfaces to form fused lamellar membranes,[15, 61, 62] while the known examples of liposome layers have been formed on TiO_2 and oxidized gold surfaces.[15, 16] Indeed, the importance of the surface chemistry in switching between the formation of flat lamellar or liposome layers has been already highlighted in early works.[16] The role of surface roughness is less clear. On one hand, it was reported to exert a considerable influence on the spreading of bilayers on solid support.[63, 64] However, other works observed that membrane formation was only little, if at all, affected by roughness in the nanometer range because the lipid membrane follows very intimately the topography of the underlying solid support, as demonstrated with membrane coating of nanoparticles.[18, 65, 66] With a simple qualitative model, the propensity of the membrane to follow the surface morphology is described by a balance between the strength of adhesion and the membrane curvature tension; thus, for weaker adhesion, the flat, partially suspended lamellar form can be a lower energy state than the curved, tightly surface bound conformation. Very minimal adhesion is sufficient to keep the membrane on the surface, even if it only acts between peaks of the substrate and a fraction of the overall surface area.

Partially suspended membrane has marked advantages over a tightly surface bound membrane when used to study protein-membrane interactions, as the full insertion of proteins typically requires some space on the support side of the membrane; and the non-zero dissipation allows the use of the main strength of the QCM-D: to analyze structural changes by using the dissipation signal. Importantly it is irrelevant that the increased dissipation is the result of out-of-plane motion or direct viscosity of the membrane, as both of these aspects are derived from mechanical ensemble properties of membranes and structural changes affect the mechanical properties. Therefore using MPA modified gold substrates offers all the advantages of a tethered membrane system without its disadvantages.

Phase transitions in supported phospholipid bilayers

The main phase transition temperature (T_m) of a phospholipid membrane is a sensitive function of the geometry and the

chemical environment[53, 67]. Hence direct measurement of T_m of supported membranes is an important indicator of their biomimetic quality. Recent works reported the use of QCM-D to measure the phase transition temperature of intact liposomes on oxide surfaces [68, 69]. Given the low dissipation of the supported membranes on metal oxide surfaces, direct measurement of the phase transition of these supported membranes was not possible using QCM. A workaround solution has been reported by using the frequency shift to identify phase transition[70]. This approach relies on the weak sensitivity of the frequency shift to the viscosity of a thin tightly coupled adlayer according to the continuum mechanical model of the QCM-D operation.[49] In light of the successful measurements of phase transition temperatures of liposomes from the change in energy dissipation[68, 69] it is preferable to detect the chain melting and concomitant viscosity change of the partially suspended membranes also from the shift in energy dissipation. Our results clearly demonstrate that such measurement is not only possible, but the phase transition temperatures of these partially suspended membranes are in a good agreement with our DSC measurements of lipid suspensions, as well as earlier literature data on dimyristoyl lipid phase transition temperatures (Table 1). Accordingly, the MPA support does not restrain lipid mobility, unlike in the case of tethering or stronger physical attachment.[39, 71] Hence, the 23.67°C identified here is the phase transition temperature of a single bilayer of DMPC.

The DMPC main phase transition is associated with chain melting, consistent with a negative shift in viscosity. Due to the identical acyl chains in the DMPC:DMPG 4:1 mixture it exhibits only small differences with respect to the pure DMPC membrane. However, inserting cholesterol into the DMPC membrane leads to more ordered lipid acyl chain conformations that eventually reduce the viscosity change upon chain melting. Accordingly the results are in a good qualitative agreement with the expected viscoelastic behaviour of these lipid mixtures.

The sensitivity of the method allows for further analysis of the membrane properties in the proximity of phase transition for the lipid mixtures. While the DMPC:DMPG bilayer shows similar behaviour to the neat DMPC bilayer, the measured phase transition temperature is somewhat higher (23.95°C vs. 23.67°C) which can be attributed to the change in headgroup packing when adding phosphatidylglycerol to a phosphatidylcholine membrane, which was shown before to change the overall bending rigidity of the membrane.[72] Furthermore, Fig. 2C shows that the dissipation decreases with two units by the end of the temperature sweep, suggesting the removal or fusion of some intact vesicles trapped within or on the top of the DMPC:DMPG bilayer upon scanning through the phase transition temperature.

The effect of cholesterol is more complex. It is generally acknowledged that cholesterol affects lipid organization, phase behaviour and membrane fluidity, and it is known to play a significant role in regulating the physical properties of the cell membrane.[73-75] The slopes in the dissipation trends in Figures 2E,G and I suggest two different viscosity trends as a function of temperature $\nu_{(T)}$. The transition between the two $\nu_{(T)}$ trends does not follow a melting profile. It is possible that the corner point in Fig. 2G reveals a sudden change in the packing order of the layer that correlates better to different polymorphs than to different thermodynamic phases. However it is also possible that the profile is the result of two overlapping phase transition peaks for two distinct phospholipid-cholesterol mixtures coexisting as separate domains in the bilayer, which is consistent with the multi-peak structure of the dD/dT profiles of Fig. 2F and Fig. 2J. It is known that incorporation of a low concentration of cholesterol (2 to 20 mol %) can lead to the formation of cholesterol-rich and cholesterol-poor domains in PC bilayer membranes[43, 76]. The formation of such domains has been also linked to the chemical nature of the substrate.[74] Our results suggest that such domains are present in a supported single bilayer membrane, and thus the QCM-D method is sensitive enough to reveal the presence of these domains.

Conclusions

It has been established that liposome deposition leads to the formation of a partially suspended membrane on MPA modified gold surface, as opposed to the tightly bound layers formed on metal oxide surfaces. The increased freedom of motion leads to a measurable dissipation signal in QCM-D experiments, which is similar to that of liposome deposits. It was found that, of the lipid mixtures studied, the addition of both hydrophilic DMPG and hydrophobic cholesterol lead to an increase in membrane viscosity, which was found to increase proportionally with cholesterol content in the 5-15% range. Moreover, the results explain the differences between single layer membrane masses reported in the literature, and demonstrate that the full potential of QCM-D in data mining the dissipation signal may be utilized for experiments on single bilayer membranes. This utility was demonstrated by determining the phase transition temperatures of membrane mixtures from the viscosity change upon chain melting. For cholesterol containing lipids it was found that the main transition is suppressed over 10% cholesterol content.

Acknowledgement

The authors acknowledge Patrick Daniel Moore for DSC measurements.

Notes and references

[a]*Department of Chemistry and Physics, School of Molecular Sciences, La Trobe University, Melbourne, Australia.*
**corresponding author. E-mail: a.mechler@latrobe.edu.au*

1. K. F. Wang, R. Nagarajan and T. A. Camesano, *Colloids and Surfaces B-Biointerfaces*, 2014, **116**, 472-481.
2. A. Coutable, C. Thibault, J. Chalmeau, J. M. Francois, C. Vieu, V. Noireaux and E. Trevisiol, *Langmuir*, 2014, **30**, 3132-3141.
3. W. C. Liao and J. A. A. Ho, *Biosens. Bioelectron.*, 2014, **55**, 32-38.
4. S. J. Ye, H. C. Li, F. Wei, J. Jasensky, A. P. Boughton, P. Yang and Z. Chen, *J. Am. Chem. Soc.*, 2012, **134**, 6237-6243.
5. B. Seantier, C. Breffa, O. Felix and G. Decher, *J. Phys. Chem. B*, 2005, **109**, 21755-21765.
6. E. Kalb, S. Frey and L. K. Tamm, *Biochimica Et Biophysica Acta*, 1992, **1103**, 307-316.
7. G. J. Hardy, R. Nayak and S. Zauscher, *Curr. Opin. Colloid Interface Sci.*, 2013, **18**, 448-458.
8. S. Subramaniam, N. L. Thompson, L. K. Tamm and H. M. McConnell, *Biophys. J.*, 1985, **47**, A367-A367.

9. N. Hain, M. Gallego and I. Reviakine, *Langmuir*, 2013, **29**, 2282-2288.
10. P. Plunkett, B. A. Camley, K. L. Weirich, J. Israelachvili and P. J. Atzberger, *Soft Matter*, 2013, **9**, 8420-8427.
11. T. Zhu, F. Xu, B. Yuan, C. L. Ren, Z. Y. Jiang and Y. Q. Ma, *Colloids and Surfaces B-Biointerfaces*, 2012, **89**, 228-233.
12. T. Tumolo, M. Nakamura, K. Araki and M. S. Baptista, *Colloids and Surfaces B-Biointerfaces*, 2012, **91**, 1-9.
13. H. Xie, K. Jiang and W. Zhan, *Physical Chemistry Chemical Physics*, 2011, **13**, 17712-17721.
14. J. T. Woodward and C. W. Meuse, *J. Colloid Interface Sci.*, 2009, **334**, 139-145.
15. C. A. Keller and B. Kasemo, *Biophysical Journal*, 1998, **75**, 1397-1402.
16. E. Reimhult, F. Hook and B. Kasemo, *Langmuir*, 2003, **19**, 1681-1691.
17. R. Richter, A. Mukhopadhyay and A. Brisson, *Biophys. J.*, 2003, **85**, 3035-3047.
18. R. P. Richter, R. Berat and A. R. Brisson, *Langmuir*, 2006, **22**, 3497-3505.
19. H. Egawa and K. Furusawa, *Langmuir*, 1999, **15**, 1660-1666.
20. M. C. Giocondi, L. Pacheco, P. E. Milhiet and C. Le Grimellec, *Ultramicroscopy*, 2001, **86**, 151-157.
21. P. E. Milhiet, V. Vie, M. C. Giocondi and C. Le Grimellec, *Single Molecules*, 2001, **2**, 109-112.
22. I. Reviakine, A. Simon and A. Brisson, *Langmuir*, 2000, **16**, 1473-1477.
23. A. Mechler, S. Praporski, S. Piantavigna, S. M. Heaton, K. N. Hall, M. I. Aguilar and L. L. Martin, *Biomaterials*, 2009, **30**, 682-689.
24. R. Liu, *Bioinspired Biomimetic and Nanobiomaterials*, 2014, **3**, 58-62.
25. M. R. Nussio, R. D. Lowe, N. H. Voelcker, B. S. Flavel, C. T. Gibson, M. J. Sykes, J. O. Miners and J. G. Shapter, *Soft Matter*, 2010, **6**, 2193-2199.
26. K. O. Evans, *Thin Solid Films*, 2012, **520**, 3026-3030.
27. B. Seantier, C. Breffa, O. Felix and G. Decher, *Nano Letters*, 2004, **4**, 5-10.
28. S. Piantavigna, G. A. McCubbin, S. Boehnke, B. Graham, L. Spiccia and L. L. Martin, *Biochimica Et Biophysica Acta-Biomembranes*, 2011, **1808**, 1811-1817.
29. K. O. Evans, *J. Phys. Chem. B*, 2008, **112**, 8558-8562.
30. A. Coutable, C. Thibault, J. Chalmeau, J. M. François, C. Vieu, V. Noireaux and E. Trévisiol, *Langmuir*, 2014, **30**, 3132-3141.
31. M. Tanaka, F. F. Rossetti and S. Kaufmann, *Biointerphases*, 2008, **3**, FA12-FA16.
32. A. Kibrom, R. F. Roskamp, U. Jonas, B. Menges, W. Knoll, H. Paulsen and R. L. C. Naumann, *Soft Matter*, 2011, **7**, 237-246.
33. H. Song, E. K. Sinner and W. Knoll, *Biointerphases*, 2007, **2**, 151-158.
34. R. Naumann, T. Baumgart, P. Graber, A. Jonczyk, A. Offenhausser and W. Knoll, *Biosens. Bioelectron.*, 2002, **17**, 25-34.
35. F. Meiners, J. H. Ross, I. Brand, A. Buling, M. Neumann, P. J. Koster, J. Christoffers and G. Wittstock, *Colloids and Surfaces a-Physicochemical and Engineering Aspects*, 2014, **449**, 31-41.
36. R. L. C. Naumann and W. Knoll, *Biointerphases*, 2008, **3**, FA101-FA107.
37. W. Knoll, I. Koper, R. Naumann and E. K. Sinner, *Electrochim. Acta*, 2008, **53**, 6680-6689.
38. D. E. Minner, V. L. Herring, A. P. Siegel, A. Kimble-Hill, M. A. Johnson and C. A. Naumann, *Soft Matter*, 2013, **9**, 9643-9650.
39. H. Basit, A. Van der Heyden, C. Gondran, B. Nysten, P. Dumy and P. Labbe, *Langmuir*, 2011, **27**, 14317-14328.
40. H. A. Eisenhauer, S. Shames, P. D. Pawelek and J. W. Coulton, *Journal of Biological Chemistry*, 2005, **280**, 30574-30580.
41. M. L. Wagner and L. K. Tamm, *Biophys. J.*, 2000, **79**, 1400-1414.
42. G. Krishna, J. Schulte, B. A. Cornell, R. J. Pace and P. D. Osman, *Langmuir*, 2003, **19**, 2294-2305.
43. T. P. W. McMullen and R. N. McElhaney, *Biochimica Et Biophysica Acta-Biomembranes*, 1995, **1234**, 90-98.
44. C. K. Park, F. J. Schmitt, L. Evert, D. K. Schwartz, J. N. Israelachvili and C. M. Knobler, *Langmuir*, 1999, **15**, 202-206.
45. K. Hall, T. H. Lee, A. I. Mechler, M. J. Swann and M. I. Aguilar, *Scientific Reports*, 2014, **4**.
46. T. H. Lee, C. Heng, M. J. Swann, J. D. Gehman, F. Separovic and M. I. Aguilar, *Biochimica Et Biophysica Acta-Biomembranes*, 2010, **1798**, 1977-1986.
47. S. Boudard, B. Seantier, C. Breffa, G. Decher and O. Felix, *Thin Solid Films*, 2006, **495**, 246-251.
48. G. Khelashvili, G. Pabst and D. Harries, *Journal of Physical Chemistry B*, 2010, **114**, 7524-7534.
49. M. V. Voinova, M. Rodahl, M. Jonson and B. Kasemo, *Phys Scripta*, 1999, **59**, 391-396.
50. L. R. Arriaga, I. Lopez-Montero, F. Monroy, G. Orts-Gil, B. Farago and T. Hellweg, *Biophysical Journal*, 2009, **96**, 3629-3637.
51. B. A. Bruning, S. Prevost, R. Stehle, R. Steitz, P. Falus, B. Farago and T. Hellweg, *Biochimica Et Biophysica Acta-Biomembranes*, 2014, **1838**, 2412-2419.
52. C. L. Armstrong, M. A. Barrett, A. Hiess, T. Salditt, J. Katsaras, A. C. Shi and M. C. Rheinstadter, *European Biophysics Journal with Biophysics Letters*, 2012, **41**, 901-913.
53. R. Koynova and M. Caffrey, *Bba-Rev Biomembranes*, 1998, **1376**, 91-145.
54. R. Lewis, Y. P. Zhang and R. N. McElhaney, *Biochimica Et Biophysica Acta-Biomembranes*, 2005, **1668**, 203-214.
55. R. J. Malcolmson, J. Higinbotham, P. H. Beswick, P. O. Privat and L. Saunier, *J Membrane Sci*, 1997, **123**, 243-253.
56. M. J. Blandamer, B. Briggs, P. M. Cullis, B. J. Rawlings and J. B. F. N. Engberts, *Physical Chemistry Chemical Physics*, 2003, **5**, 5309-5312.
57. H. Binder and O. Zschornig, *Chemistry and Physics of Lipids*, 2002, **115**, 39-61.
58. T. Ghodselahi, S. Hoornam, M. A. Vesaghi, B. Ranjbar, A. Azizi and H. Mobasheri, *Applied Surface Science*, 2014, **314**, 138-144.
59. A. Graneli, J. Rydstrom, B. Kasemo and F. Hook, *Langmuir*, 2003, **19**, 842-850.
60. P. Y. Peng, P. C. Chiang and L. Chao, *Acs Applied Materials & Interfaces*, 2014, **6**, 12261-12269.
61. P. Vermette, H. J. Griesser, P. Kambouris and L. Meagher, *Biomacromolecules*, 2004, **5**, 1496-1502.
62. N. Granqvist, M. Yliperttula, S. Valimaki, P. Pulkkinen, H. Tenhu and T. Viitala, *Langmuir*, 2014, **30**, 2799-2809.
63. J. Radler, H. Strey and E. Sackmann, *Langmuir*, 1995, **11**, 4539-4548.
64. P. S. Cremer and S. G. Boxer, *J. Phys. Chem. B*, 1999, **103**, 2554-2559.
65. R. P. Richter and A. Brisson, *Langmuir*, 2003, **19**, 1632-1640.
66. S. Mornet, O. Lambert, E. Duguet and A. Brisson, *Nano Letters*, 2005, **5**, 281-285.
67. R. L. Biltonen and D. Lichtenberg, *Chemistry and Physics of Lipids*, 1993, **64**, 129-142.
68. G. Ohlsson, A. Tigerstrom, F. Hook and B. Kasemo, *Soft Matter*, 2011, **7**, 10749-10755.
69. P. Losada-Perez, K. L. Jimenez-Monroy, B. van Grinsven, J. Leys, S. D. Janssens, M. Peeters, C. Glorieux, J. Thoen, K. Haenen, W. De Ceuninck and P. Wagner, *Physica Status Solidi a-Applications and Materials Science*, 2014, **211**, 1377-1388.
70. A. Wargenau and N. Tufenkji, *Analytical Chemistry*, 2014, **86**, 8017-8020.
71. D. Dutta and L. C. Kam, in *Micropatterning in Cell Biology, Pt B*, eds. M. Piel and M. Thery, 2014, vol. 120, pp. 53-67.
72. M. Claessens, B. F. van Oort, F. A. M. Leermakers, F. A. Hoekstra and M. A. C. Stuart, *Physical Review E*, 2007, **76**.
73. R. S. Gracia, N. Bezlyepkina, R. L. Knorr, R. Lipowsky and R. Dimova, *Soft Matter*, 2010, **6**, 1472-1482.

74. R. Lipowsky, T. Rouhiparkouhi, D. E. Discher and T. R. Weikl, *Soft Matter*, 2013, **9**, 8438-8453.
75. B. Bruning, M. Rheinstadter, A. Hiess, B. Weinhausen, T. Reusch, S. Aeffner and T. Salditt, *Eur Phys J E*, 2010, **31**, 419-428.
76. A. Hodzic, M. Rappolt, H. Amenitsch, P. Laggner and G. Pabst, *Biophysical Journal*, 2008, **94**, 3935-3944.